www.czasopisma.pan.pl PAN www.journals.pan.pl
Chemical and Process Engineering 2019, 40 (1), 101–114
DOI: 10.24425/cpe.2019.126104

# Heat transfer in helical coil heat exchanger: An experimental parametric study

Krzysztof Kowalski, Dorota Downarowicz*

West Pomeranian University of Technology, Szczecin, Faculty of Chemical Technology and Engineering, Institute of Chemical Engineering and Environmental Protection Processes, al. Piastów 42, 71-065 Szczecin, Poland

Helical coil heat exchangers are widely used in a variety of industry applications such as refrigeration systems, process plants and heat recovery. In this study, the effect of Reynolds number and the operating temperature on heat transfer coefficients and pressure drop for laminar flow conditions was investigated. Experiments were carried out in a shell and tube heat exchanger with a copper coiled pipe (4 mm ID, length of 1.7 m and coil pitch of 7.5 mm) in the temperature range from 243 to 273 K. Air – propan-2-ol vapor mixture and coolant (methylsilicone oil) flowed inside and around the coil, respectively. The fluid flow in the shell-side was kept constant, while in the coil it was varied from 6.6 to 26.6 m/s (the Reynolds number below the critical value of 7600). Results showed that the helical pipe provided higher heat transfer performance than a straight pipe with the same dimensions. The convective coefficients were determined using the Wilson method. The values for the coiled pipe were in the range of 3–40 W/m$^2$·K. They increased with increasing the gas flow rate and decreasing the coolant temperature.

**Keywords:** helical coil, heat exchanger, condensation, Wilson method, laminar flow, pressure drop

## 1. INTRODUCTION

A helical coil heat exchanger consists of a cylindrical shell and a helical coiled tube with constant curvature ratio and coil pitch. It is widely used in various industrial applications due to its simple and compact structure, especially when a large heat exchange area is not required (Błasiński and Młodziński, 1983; Bejan and Kraus, 2003). The heat exchanger is one of the key devices in chemical, petroleum, refrigeration, food, power generation and nuclear industries as well as in air-conditioning and heat recovery systems. It can be used in sterilization, pasteurization, cryogenic, crystallization, separation (distillation) and reaction processes (Nada et al., 2016; Pandey et al., 2015).

The flow and convective heat transfer in a helical coiled tube are more complex than in a straight tube, because they strongly depend on the behavior of secondary flow, which enhances the heat transfer rate and fluid mixing. This phenomenon is particularly distinct in the laminar flow regime (Jayakumar, 2012; Ju et al., 2001).

In a straight pipe, the velocity profile of laminar flow is parabolic, because viscous forces are larger than inertial forces and are enough to suppress fluid fluctuations. When the fluid flows through a coiled tube, the

* Corresponding author, e-mail: ddownar@zut.edu.pl

*Reprinted with permission in an extended form from the EYEC Monograph accompanying 7th European Young Engineers Conference.* 

main (primary) velocity profile is distorted due to the formation of a secondary flow induced by centrifugal forces (Ghias et al., 2016). This flow is produced in the plane perpendicular to the axial flow direction.

Coil curvature ratio and the Reynolds number govern the flow in coiled tubes. The former parameter is defined as the ratio of coil to tube diameters, whereas the other as the ratio of inertia to viscous forces (Pandey et al., 2015). The Dean ($De$) number is the product of the Reynolds number and the square root of the curvature ratio. The inertial forces are negligible for low Dean numbers ($De < 20$). They are balanced by the viscous forces in the intermediate Dean value range ($20 < De < 40$). In other cases, viscous forces are significant only in the boundary near the tube wall. Pressure drop in helical coils at low values of Reynolds number is highly dependent on curvature ratio. As the flow rate increases, the effect of curvature ratio on the pressure drop decreases (Vashisth et al., 2008).

The helical coil heat exchangers can be applied for the separation of solvent vapors from gas stream in air purification plants. However, to date very few studies have addressed this issue. The knowledge of the heat transfer and flow characteristics is essential to design and optimization of such devices (Alimoradi, 2017; Naphon and Wongwises, 2006). In optimal conditions the heat transfer coefficient should be as high as possible with the lowest possible pressure drop. These coefficients can be determined from various Nusselt number correlations developed for specific geometries of coil heat exchangers and fluid flow regimes. The Wilson plot method delivers an estimation procedure of convective coefficients in the coil heat exchangers based on experimental measurements of hot and cold fluid flow rates and their inlet and outlet temperatures in steady-state conditions (Van Rooyen, 2011). Therefore, measurements of coil surface temperatures are not required. This is the main advantage of the method because it is difficult to accurately measure these temperatures (Sobota, 2011). The main objective of this study was to investigate the influence of gas flow rate and the operating temperature on the heat transfer performance and the pressure drop in the helical coil heat exchanger which was used to cool vapour-air mixtures. Heat transfer coefficients were determined using the Wilson method and from Nusselt number correlations for laminar flow regime.

## 2. EXPERIMENTAL SETUP

### *2.1. Apparatus and materials*

Figure 1 shows a schematic diagram of the experimental setup. The setup consists of a gas preparation section, a helical coil heat exchanger, a refrigerated circulator (FP ME50, Julabo) and a data acquisition system. The schematic diagram of the coil heat exchanger and its geometry parameters are shown in Fig. 2 and Tab. 1, respectively.

The construction of the heat exchanger is shown in Fig. 2. Pure or 2-propanol (IPA)-laden air streams with specified concentrations ranging from 3.9 to 10.4 g/m$^3$ were used in the study. Experiments were performed in the following invariability range of operating parameters: air velocity 6.6–26.6 m/s and the coolant temperature 243–273 K. The measurements were conducted at ambient laboratory temperature (297–301 K).

As can be seen from Fig. 1, vapor-gas mixture was produced by mixing IPA with air in the gas preparation section. Compressed air was passed through desiccant dryers (Kaeser, DC 1.5–7.5) in order to minimize the effect of moisture during the experiments. Dried air stream was passed through the organic vapor generator (static mixer with an external heating cord) while liquid IPA was injected into the gas stream using a syringe pump (model 100, KD Scientific, accuracy: ±1%). The gas flow rate was measured with a mass flow controller (model GFC 47, Aalborg, accuracy: ±1%). The resulting hot gas mixture was cooled to ambient temperature in a water cooler and then passed through a copper coil pipe in the heat exchanger.

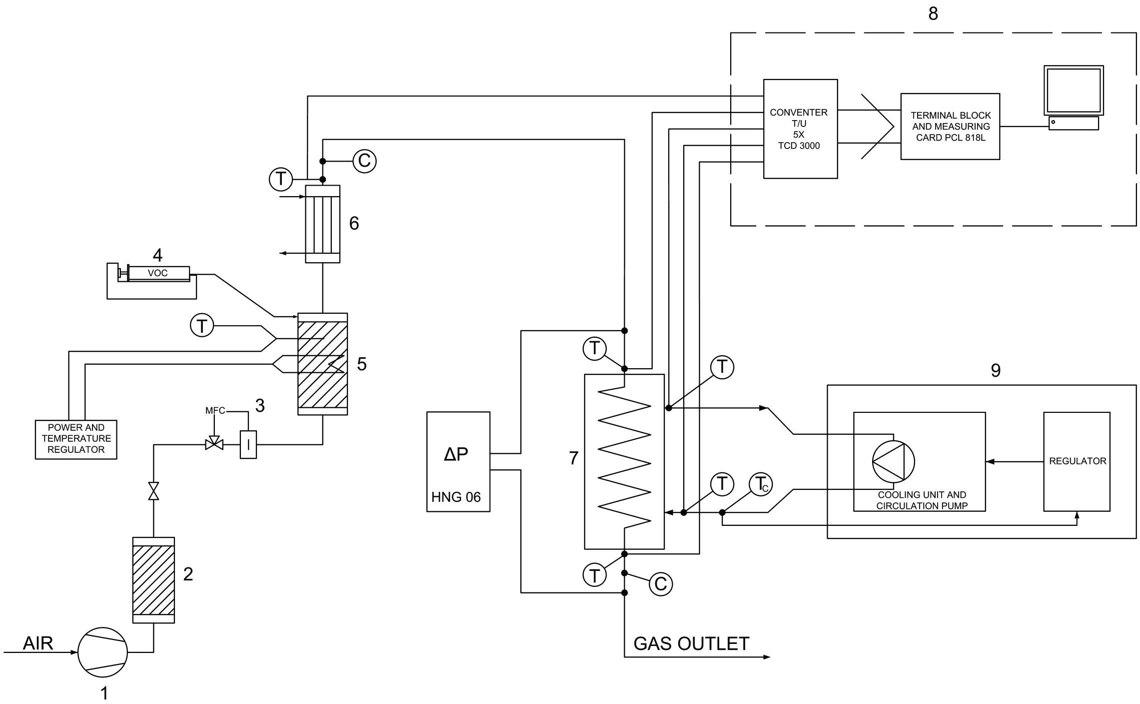


Fig. 1. Schematic diagram of experimental setup; 1 – compressor, 2 – desiccant dryers, 3 – flowmeter, 4 – VOC syringe pump, 5 – static mixer, 6 – water cooler, 7 – coil heat exchanger, 8 – data acquisition system, 9 – refrigerated circulator, T – temperature sensor, $T_C$ – Pt100 sensor, C – sampling point

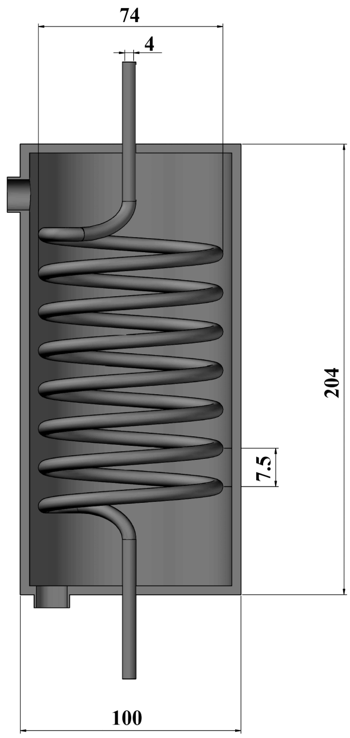


Fig. 2. Geometry of heat exchanger

Pure or isopropanol (IPA)-laden air streams with specified concentrations ranging from 3.9 to 10.4 g/m$^3$ were used in the study. The IPA vapor concentration stability was monitored using a gas chromatograph (SRI 8610C) with a flame ionization detector (FID). The cooling medium (methylsilicone oil) circulated through an external loop of the FP ME50 circulator and flowed outside the coil (inside the shell). For highly precise control of the outlet oil temperature, an external Pt100 sensor ($T_C$) was installed directly into the

Table 1. Geometry parameters of the heat exchanger

| Parameters | Value |
|---|---|
| Inner diameter of coiled tube ($d_{in}$) | 4 mm |
| Tube thickness | 1 mm |
| Coil diameter ($D$) | 74 mm |
| Tube length ($L$) | 1700 mm |
| Coil pitch ($p_t$) | 7.5 mm |
| Curvature ratio $\left(\delta = \dfrac{D}{d_{in}}\right)$ | 18.5 |

loop circuit of the refrigerated circulator (temperature stability: ±0.01 °C). The efficiency of the circulator pump was automatically adjusted with bath fluid viscosity changes caused by temperature change. Inlet and outlet temperatures of both working fluids were measured with K-type thermocouples (1 mm O.D, class 1) placed in the pipe axis. DASYLab (National Instruments, Ireland) software was used in a data acquisition system to record temperature data with a 1 s sampling rate. Tests were conducted until the steady-state was reached, indicated by a stable gas outlet temperature. Accuracy of temperature measurements was ±0.5%.

The HGM1 type differential pressure gauge (Kalinsky Sensor Elektronik GmbH & Co., accuracy: ±0.8%) was used to measure the differential pressure through the coil pipe.

### *2.2. Flow characteristics of helical coil heat exchanger*

The Dean number is a characteristic parameter for flow in a helical tube, like the Reynolds number for flow in a straight pipe. The numbers are defined as follows:

$$De = Re\sqrt{\frac{d_{in}}{D}} \tag{1}$$

$$Re = \frac{4G}{\pi d_{in}\mu} \tag{2}$$

The Dean number characterizes the strength of secondary flow, which is perpendicular to the main flow direction (Fig. 3) and enhances fluid mixing. The centrifugal force exerted by a pipe curvature causes this phenomenon (Ju et al., 2001; Kocatepe et al., 2009).

In the investigated air flow range, the values of the $Re$ and $De$ numbers ranged from 1670 to 7500 and from 390 to 1750, respectively. The critical Reynolds number ($Re_{cr}$) is defined as the maximum value of the Reynolds number for which the flow in a coil pipe is still laminar. The following empirical equations are commonly used to define of $Re_{cr}$ in laminar flow region:

- Ito equation (Flórez-Orregoa et al., 2012):

$$Re_{cr} = 2000\left[1 + 13.2\,\delta^{-0.6}\right] \quad \text{for} \quad 5 \le \delta \le 2000, \tag{3}$$

  where $\delta$ is a curvature ratio.

- Srinivasan equation (Flórez-Orregoa et al., 2012; Srinivasan et al. 1968):

$$Re_{cr} = 2100\left[1 + 12\,\delta^{-0.5}\right] \quad \text{for} \quad 7.5 \le \delta \le 100 \tag{4}$$

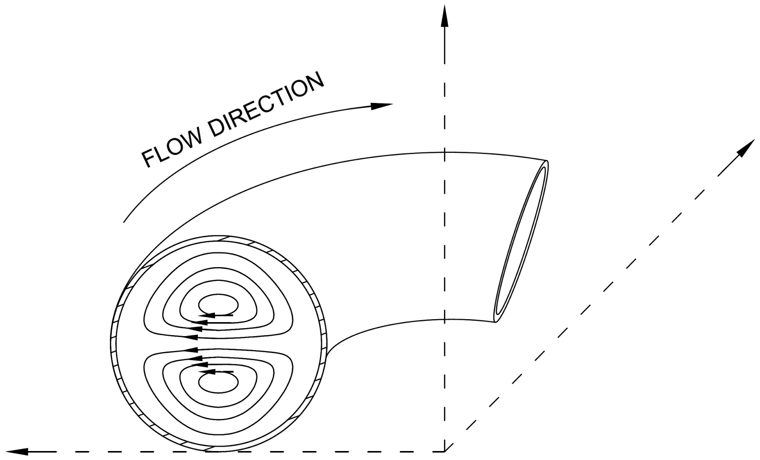


Fig. 3. The secondary flow pattern in a helical pipe

- Cioncolini equation (Cioncolini and Santini, 2006):

$$Re_{cr} = 30000\ \delta^{-0.47} \quad \text{for} \quad 7 \le \delta \le 24 \tag{5}$$

- Schmidt equation (Vashisth et al., 2008; Schmidt, 1967):

$$Re_{cr} = 2300\left[1 + 8.6\left(\frac{d_{in}}{D}\right)^{0.45}\right] \tag{6}$$

The estimated values of the $Re_{cr}$ number are given in Tab. 2.

Table 2. Critical Reynolds values for air flow in the coil pipe

| Authors | $Re_{cr}$ |
|---|---|
| Ito | 6585 |
| Srinivasan | 7959 |
| Cioncolini | 7613 |
| Schmidt | 7619 |

As Table 2 shows, the $Re_{cr}$ number calculated from the Ito's equation is slightly lower as compared to values obtained from other equations while a value determined from the Cionciolini equation agrees well with the Schmidt's correlation. Both values are close to 7600 and are higher than the maximum Reynolds number for laminar flow in a straight pipe ($Re = 2100$) by about 3.6 times. The $Re_{cr}$ value is slightly larger than the upper limit of the test $Re$ values thus all experiments were conducted in the laminar flow region.

### *2.3. The Wilson-plot technique*

The Wilson plot technique enables determination of convective coefficients based on the overall temperature difference and the heat transfer rate. The heat transferred during the gas cooling can be determined from the following equations:

- For a single-phase IPA-air mixture (Sapali and Patil, 2010):

$$Q = \left(G_{AIR}C_{p,AIR} + G_{IPA}C_{p,IPA}\right)\left(T_{coil,out} - T_{coil,in}\right) \tag{7}$$

- For air stream (Uhía et al., 2013; Witchayanuwat and Kheawhom, 2010):

$$Q = G_{AIR} C_{p,AIR} \left( T_{coil,out} - T_{coil,in} \right) \tag{8}$$

- The overall heat exchange coefficient is defined as (Bejan and Kraus, 2003; Pettersen et al., 2000):

$$U = \frac{Q}{A_{out} \cdot LMTD} \tag{9}$$

where the log mean temperature difference (*LMTD*) in a counter flow heat exchanger can be expressed as (Shah and Sekulić, 2003):

$$LMTD = \frac{\left(T_{coil,out} - T_{shell,in}\right) - \left(T_{coil,in} - T_{shell,out}\right)}{\ln\left(\dfrac{T_{coil,out} - T_{shell,in}}{T_{coil,in} - T_{shell,out}}\right)} \tag{10}$$

The total thermal resistance is the inverse of the overall heat transfer coefficient referred to the outer pipe surface area ($A_{out}$). It can be defined as a sum of the convective resistances at the inner and outer sides of the coil pipe and of the wall conduction resistance (Sobota, 2011; Kumbhare et al., 2012):

$$\frac{1}{UA_{out}} = \frac{1}{\alpha_{in} A_{in}} + \frac{\ln\left(\dfrac{d_{out}}{d_{in}}\right)}{2\pi \lambda_{wall} L} + \frac{1}{\alpha_{out} A_{out}} \tag{11}$$

In the coil heat exchanger, the coolant flow rate was constant, while the gas stream velocity was varied. By keeping the mass flow rate in the shell constant, it is then assumed that the shell side heat transfer coefficient is constant (Jamshidi et al., 2013; Kumar et al., 2007).

In this case, the values of total thermal resistance depend on the change in the internal heat transfer coefficient, while the remaining thermal resistances remain almost constant (Shiragami and Inoue, 1986). Therefore, the sum of the convective resistances of the outside coil tube and in the tube wall can be expressed as (Sobota, 2011; Yang and Chiang, 2002):

$$C_1 = \frac{1}{\alpha_{out}} + \frac{A_{out} \ln\left(\dfrac{d_{out}}{d_{in}}\right)}{2\pi \, \lambda_{wall} \, L} \tag{12}$$

The internal heat transfer coefficient ($\alpha_{in}$) can be calculated from the following Nusselt number correlation:

$$Nu = C \, Re^n \, Pr^{0.4} = \frac{\alpha_{in} d_{in}}{\lambda_{in}} \tag{13}$$

This general equation is applicable to the laminar as well as turbulent forced convection. When the gas mixture properties are constant, then the convective coefficient inside the tube is proportional to the $n$-th power of the fluid velocity (Shah and Sekulić, 2003; Shiragami and Inoue, 1986):

$$\alpha_{in} = C_2 w^n \tag{14}$$

Substituting Eqs. (12) and (14) into Eq. (11) results in (Shiragami and Inoue, 1986):

$$\frac{1}{U} = C_1 + \frac{C_3}{w^n} \tag{15}$$

In the Wilson technique, the plot $1/U$ versus $1/w^n$ should be linear for an assumed value of the n exponent. The $C_2$ and $C_1$ coefficients are the slope and $y$-intercept of the straight line graph. Both constants are determined using the least square fitting method. The obtained values of the best-fit parameters enable

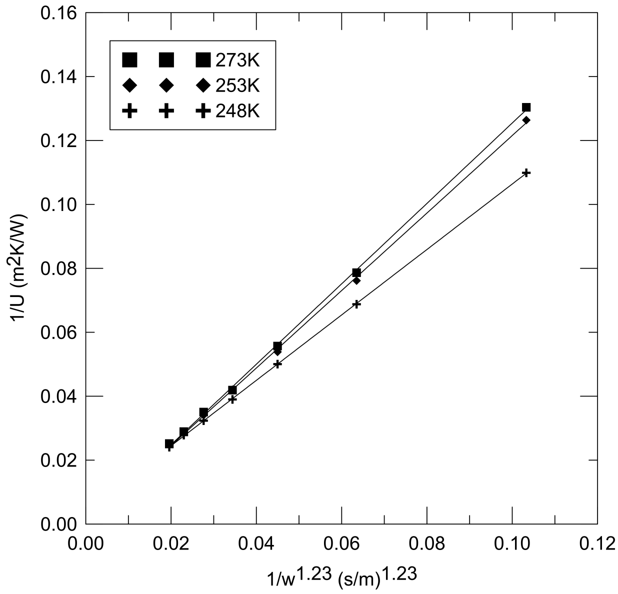


Fig. 4. The plot of inverse overall heat transfer coefficient versus inverse air velocity inside coil tube

calculating the external and internal convective coefficients for a given gas flow rate. As can be seen from Fig. 4, the experimental data are well represented by Eq. (15) for the assumed value of $n = 1.23$. The quality of the fit is very good, as proven by the high values of the determination coefficients ($R^2 > 0.999$).

The uncertainty for the experimental results was calculated based on the procedure described by Uhía et al. The maximum uncertainties are ±0.7% for the logarithmic mean temperature difference (*LMTD*), ±14.1% for the heat transfer rate ($Q$), ±7% for the Reynolds number.

An effect of the *Re* number on the internal heat transfer coefficient was presented in Fig. 5.

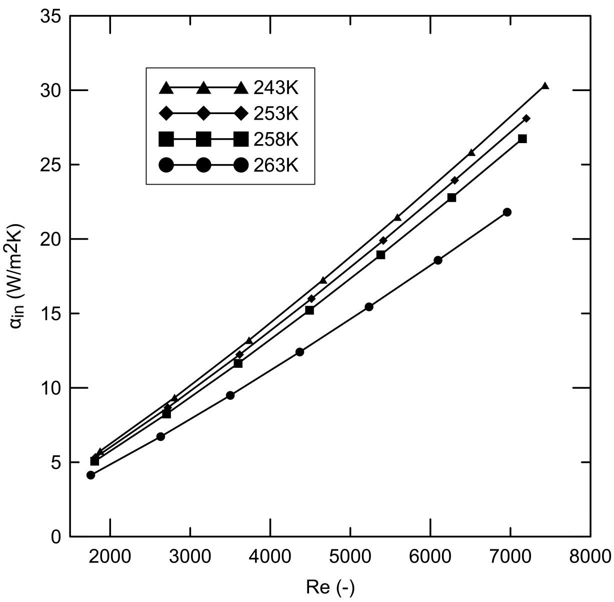


Fig. 5. The plot of inside heat transfer coefficient versus Reynolds number for air cooling

The graph legends show the values of stabilized coolant temperature in the cooling loop of the circulator for individual experimental series.

Figure 5 shows that an increase in the Reynolds numbers and a decrease in coolant temperature affect an increase in the heat transfer coefficient values. In the laminar flow regime, due to the curvature of the coil tube, a centrifugal force is generated, which produced a secondary flow. A decrease in temperature affects an increase in gas temperature difference in the exchanger. Therefore, more heat is transferred to the cold medium. These results are in agreement with the finding reported by Ghias et al. (2016).

Fig. 6 shows that the effect of the Reynolds number was stronger than the change in the gas mixture composition. As can be seen, the heat transfer coefficients for the IPA vapor concentration of 3 g/m$^3$ were very close to those for clean air and lower than those for 8 g/m$^3$ by ca. 40%. This suggests that other additional phenomena may have occurred in the coil tube. Because of the complexity of this issue, further studies are necessary to fully elucidate this process.

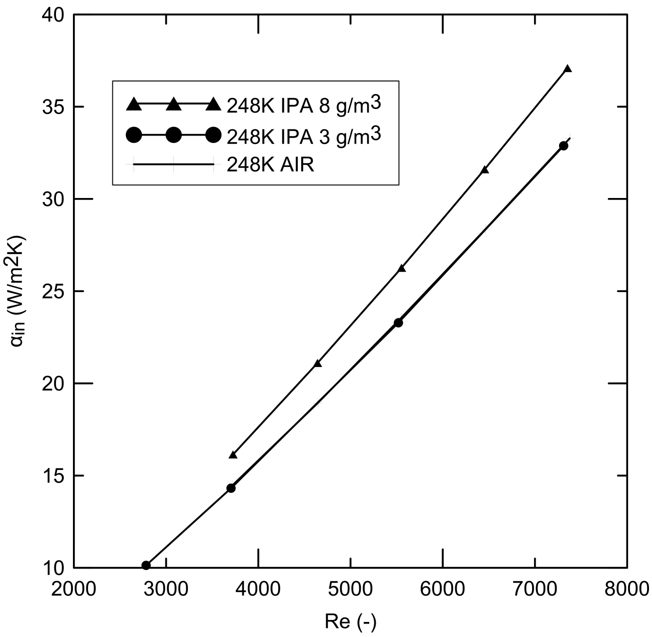


Fig. 6. Comparison between heat transfer coefficients for air and IPA-air mixture inside coil tube at 248 K

## 3. RESULTS AND DISCUSSION

The thermo-hydraulic behavior in the coil tube-side in single-phase flow was analyzed using empirical correlations of friction factor and Nusselt number. The analysis was performed by varying the Reynolds number, and consequently the Dean number.

### *3.1. Nusselt number correlations*

The effect of the coil curvature and the Reynolds number on the heat transfer efficiency in laminar flow regime was evaluated using the following Nusselt number correlations:

- Schmidt equation (Schmidt, 1967; Sobota, 2011):

$$Nu = 3.65 + 0.08\left[1 + 0.8\left(\frac{d_{in}}{D}\right)^{0.9}\right] Pr^{\frac{1}{3}} Re^{0.5+0.2903\left(\frac{d_{in}}{D}\right)^{0.194}} \quad \text{for} \quad 100 < Re < Re_{cr} \tag{16}$$

- Seban and Mclaughlin equation (Flórez-Orregoa et al., 2012):

$$Nu = 0.023\,Re^{0.8}Pr^{0.4}\left[Re^{0.05}\left(\frac{d_{in}}{D}\right)^{0.1}\right] \qquad \text{for} \quad 5000 < Re < 100000 \tag{17}$$

- Xin and Ebadian equation (Flórez-Orregoa et al., 2012):

$$Nu = 0.0019\,Re^{0.92}Pr^{0.4}\left[1 + 3.455\left(\frac{d_{in}}{D}\right)^{0.1}\right] \tag{18}$$

  when $5000 < Re < 100000$.
- Naphon and Wongwises equation (Naphon and Wongwises, 2006):

$$Nu = \left(2.153 + 0.318\,De^{0.643}\right)Pr^{0.177} \tag{19}$$

  when $20 < De < 2000$
- Kalb and Seaderequation (Naphon and Wongwises, 2006):

$$Nu = 0.836\,De^{0.5}Pr^{0.1} \qquad \text{for} \quad De \geq 80, 0.7 < Pr < 5 \tag{20}$$

As Table 3 shows, the convective heat transfer coefficients determined by Wilson's procedure are significantly lower than those calculated from empirical correlations. In the range of $Re > 5000$, the equation of Xin and Ebadian is more suitable than the others.

Table 3. Calculated *Nu* number versus *Re* number at 273 K

| Authors | *Re* [–] | | | | | | |
|---|---|---|---|---|---|---|---|
| | 1700 | 2600 | 3400 | 4200 | 5100 | 5900 | 6800 |
| | Results | | | | | | |
| Wilson | 0.80 | 1.30 | 1.84 | 2.40 | 2.99 | 3.59 | 4.21 |
| Xin and Ebadian | – | – | – | – | 4.95 | 5.67 | 6.38 |
| Seban and Mclaughlin | – | – | – | – | 7.27 | 8.28 | 9.27 |
| Schmidt | 14.48 | 17.81 | 20.77 | 23.50 | 26.04 | 28.44 | 30.73 |
| Naphon and Wongwises | 16.20 | 20.39 | 24.10 | 27.48 | 30.63 | 33.58 | 36.40 |
| Kalb/Seader | 16.18 | 19.79 | 22.83 | 25.51 | 27.93 | 30.16 | 32.23 |

### *3.2. Pressure drop in helical coiled tube*

The pressure drop of single-phase flow in a straight tube can be calculated from Darcy-Weisbach equation (Silva et al., 2001; Urbanowicz-Górska and Wojtkowiak, 2012):

$$\Delta p = f_S \frac{L \cdot w^2 \cdot \rho}{2d_{in}} \tag{21}$$

The friction factor $(f_S)$ in smooth tubes depends on the Reynolds number:

$$f_S = 64/Re \qquad \text{for} \quad Re < 2100 \tag{22}$$

$$f_S = 0.3164/Re^{1/4} \qquad \text{for} \quad 3000 < Re < 10^5 \tag{23}$$

The pressure drop in a coil tube can be calculated from Eq. (21) after replacing the friction factor $f_S$ by Fanning (coil) friction factor $f_C$ or the ratio of both friction factors $(f_S/f_C)$.

The following equations were used in the present analysis:

- Shiragami (Shiragami and Inoue, 1986):

$$f_C = f_S 0.0040 \left[ Re \left( \frac{1}{\delta} \right)^{0.2} \right]^{0.87} \qquad \text{for} \quad 1/\delta \leq 0.0729 \tag{24}$$

- Gnieliński et al. (Silva et al., 2001):

$$f_C = \left( 1.82 \log Re^{-1.64} \right)^{-2} \tag{25}$$

- Ito (Gupta et al., 2011):

$$f_C = f_S \left( 0.1033 \sqrt{De} \left[ \left( 1 + \frac{1.729}{De} \right)^{0.5} - \left( \frac{1.729}{De} \right)^{0.5} \right]^{-3} \right) \tag{26}$$

- Manlapaz and Churchill (Urbanowicz-Górska and Wojtkowiak, 2012) suggested a correlation valid in the wide range of the Dean number:

$$f_C = f_S \left( 1 + \left( 1 + \frac{d_{in}}{3D} \right)^2 \frac{De}{88.33} \right)^{0.5} \qquad \text{for} \quad De < 40 \tag{27}$$

- Mishra and Gupta (Gupta et al., 2011):

$$f_C = f_S \left( 1 + 0.033 \left( \log_{10} He \right)^4 \right) \qquad \text{for} \quad 1 < He < 3000 \tag{28}$$

  where $He$ is the Helix number defined as

$$He = De \left[ 1 + \left( \frac{p_t}{2\pi D} \right)^2 \right]^{1/2} \tag{29}$$

Table 4 shows a comparison of the pressure drop values determined from the Darcy-Weisbach equation with experimental data obtained for the same dimensions of the pipe.

Table 4. Pressure drops versus the $Re$ number in the laminar flow regime ($Re < 2100$)

| Air flow [m$^3$/h] | $Re$ [–] | Pressure drop [Pa] | | |
|---|---|---|---|---|
| | | Experiment | Straight pipe | Coiled pipe |
| 0.03 | 157 | 238 | 42 | 50 |
| 0.04 | 220 | 289 | 58 | 75 |
| 0.06 | 315 | 400 | 83 | 117 |
| 0.08 | 409 | 442 | 108 | 163 |
| 0.09 | 472 | 489 | 125 | 197 |
| 0.10 | 535 | 595 | 142 | 232 |
| 0.12 | 630 | 650 | 167 | 288 |
| 0.13 | 693 | 716 | 183 | 328 |
| 0.15 | 787 | 787 | 208 | 389 |
| 0.16 | 850 | 920 | 225 | 432 |
| 0.18 | 945 | 957 | 250 | 499 |

The friction factors were predicted from Eqs. (22) and (26) that were developed for straight and coiled pipes, respectively. As can be seen, the values of the pressure drop are underestimated in comparison to experimental data (average relative errors were 329% and 176%, respectively). Therefore, it may be concluded that both equations are not appropriate to predict the pressure drop inside the coiled pipe in a low Re number range.

As seen in Table 5, the friction factors calculated from Eqs. (26)–(28) were close together for the same *Re* numbers. The Gnieliński equation provided the best agreement of the results with those obtained from the Blasius correlation. In contrast to the Eq. (24), the values calculated from the other equations decrease with increasing the *Re* number.

Table 5. Friction factor values versus the *Re* number ($Re > 3000$)

| Air flow [$m^3$/h] | *Re* [–] | Blasius (Eq. (23)) | Shirigami (Eq. (24)) | Gnieliński (Eq. (25)) | Ito (Eq. (26)) | Manlapaz/ Churchill (Eq. (27)) | Mishra/ Gupta (Eq. (28)) |
|---|---|---|---|---|---|---|---|
| 0.60 | 3334 | 0.041 | 0.034 | 0.044 | 0.063 | 0.059 | 0.063 |
| 0.75 | 4163 | 0.039 | 0.040 | 0.041 | 0.055 | 0.053 | 0.055 |
| 0.90 | 4992 | 0.038 | 0.045 | 0.038 | 0.050 | 0.048 | 0.050 |
| 1.05 | 5821 | 0.036 | 0.050 | 0.037 | 0.046 | 0.044 | 0.045 |
| 1.20 | 6649 | 0.035 | 0.054 | 0.035 | 0.043 | 0.041 | 0.042 |
| | | Approximation error | | | | | |
| | | 20% | 31% | 18% | 12% | 11% | 11% |

Based on the data analysis for $Re < 2100$, it can be assumed that Eqs. (26)–(28) give more reliable results than those obtained from Eqs. (24) and (25) and may be used to evaluate pressure drops in the coiled tube in laminar regime.

## 4. CONCLUSION

The main objective of the present work was to study the impact of the Reynolds number and coolant (methylsilicone oil) temperature on the heat transfer coefficient in a helical coil exchanger with an air-propan-2-ol vapor mixture as the working medium. The Wilson plot method was used for determining convective coefficients based on experimental measurements in steady-state conditions. Data analysis revealed that the decrease in the temperature by 25 K resulted in the increase of the heat transfer coefficients by ca. 10%. While, a threefold increase in the gas flow rate affected an increase in value by ca. 80%. The coefficient values for clean air did not exceed 40 W·$m^2$/K.

The observed heat transfer performance enhancement was due to the more efficient mixing of fluids induced by the centrifugal force in the coil tube, which resulted in secondary flow development. This phenomenon is responsible for higher frictional pressure drop in the coiled pipe than in the straight tube with the same dimensions.

Due to the lack of general correlations for whole geometrical and flow conditions, several empirical equations were selected to calculate the *Nu* number and the pressure drop inside the coiled pipe. A comparison between experimental and calculated results for the same Reynolds number showed that the predicted data were overestimated and prediction accuracy was dependent on the fluid flow conditions. Therefore, the usefulness of these equations for designing helical coil heat exchangers was very limited.

## SYMBOLS

| | |
|---|---|
| $A$ | coil area, m$^2$ |
| $C$ | constant, – |
| $C_1$ | constant, – |
| $C_2$ | constant, – |
| $C_3$ | constant, – |
| $C_p$ | heat capacity, J/(kg·K) |
| $D$ | coil dimension, m |
| $De$ | Dean number, – |
| $d$ | pipe dimension, m |
| $f$ | friction factor, – |
| $g$ | standard gravity, m/s$^2$ |
| $G$ | mass flow, kg/s |
| $He$ | Helix number, – |
| $L$ | coil length, m |
| $LMTD$ | logarithmic mean temperature difference, K |
| $n$ | coefficient, – |
| $Nu$ | Nusselt number, – |
| $Pr$ | Prandtl number, – |
| $p_t$ | coil pitch, m |
| $Q$ | heat flow, W |
| $Re$ | Reynolds number, – |
| $Re_{cr}$ | critical Reynolds number, – |
| $T$ | temperature, K |
| $U$ | overall heat transfer coefficient, W/(m$^2$·K) |
| $w$ | gas velocity, [m/s] |

*Greek symbols*

| | |
|---|---|
| $\alpha$ | heat transfer coefficient, W/(m$^2$·K) |
| $\delta$ | curvature ratio, – |
| $\Delta p$ | pressure drop, Pa |
| $\lambda$ | thermal conductivity, W/(m·K) |
| $\mu$ | viscosity, Pa·s |
| $\rho$ | density, kg/m$^3$ |

*Subscripts*

| | |
|---|---|
| $in$ | inside |
| $out$ | outside |
| $c$ | curved tube |
| $s$ | straight tube |

## REFERENCES

Alimoradi A., 2017. Study of thermal effectiveness and its relation with NTU in shell and helically coiled tube heat exchangers. *Case Stud. Therm. Eng.*, 9, 100–107. DOI: 10.1016/j.csite.2017.01.003.

Bejan A., Kraus A., 2003. *Heat transfer handbook*. John Wiley & Sons, Inc., Hoboken.

Błasiński M., Młodziński B., 1983. *Aparatura przemysłu chemicznego*. Wydawnictwa Naukowo-Techniczne, Warszawa.

Cioncolini A., Santini L., 2006. An experimental investigation regarding the laminar to turbulent flow transition in helically coiled pipes. *Exp. Therm Fluid Sci.*, 30, 367–380. DOI: 10.1016/j.expthermflusci.2005.08.005.

Flórez-Orregoa D., Ariasa W., Lópeza D., Velásqueza H., 2012. Experimental and CFD study of a single phase cone-shaped helical coiled heat exchanger: an empirical correlation, In: Sciubba E., Manfrida G., Desideri U. (Eds.), *ECOS 2012 The 25th International Conference on Efficiency, Cost, Optimization and Simulation of Energy Conversion Systems and Processes*. Firenze University Press. ID 375.

Ghias A.S.A., Ananth S.V., Anand M.D., Devadhas G.G., 2016. Experimental study of thermal performance of coil in shell heat exchanger. *Indian J. Sci. Technol.*, 9, 1–17. DOI: 10.17485/ijst/2016/v9i13/90571.

Gupta R., Wanchoo R.K., Jafar Ali T.R.M., 2011. Laminar flow in helical coils: a parametric study. *Ind. Eng. Chem. Res.*, 50, 1150–1157. DOI: 10.1021/ie101752z.

Jamshidi N., Farhadi M., Ganji D., Sedighi K., 2013. Experimental analysis of heat transfer enhancement in shell and helical tube heat exchangers. *Appl. Therm. Eng.*, 51, 644–652. DOI: 10.1016/j.applthermaleng.2012.10.008.

Jayakumar J.S., 2012. *Helically coiled heat exchangers*. INTECH Open Access Publisher.

Ju H., Huang Z., Xu Y., Duan B., Yu Y., 2001. Hydraulic performance of small bending radius helical coil-pipe. *J. Nucl. Sci. Technol.*, 38, 826–831. DOI: 10.1080/18811248.2001.9715102.

Kocatepe Y., Ahn H., Aydin C., Karacasu A., 2009. Experimental investigation of a heat exchanger with a helical coil made of corrugated tubes. *17. National Thermal Science and Technology Congress (ULIBTK'09).* Cumhuriyet University, Sivas, 24 June 2009.

Kumar V., Mridha M., Gupta A., Nigam K., 2007. Coiled flow inverter as a heat exchanger. *Chem. Eng. Sci.*, 62, 2386–2396. DOI: 10.1016/j.ces.2007.01.032.

Kumbhare B.P., Purandare P.S., Mali K.V., 2012. Experimental analysis of square and circular helical coil for the heat recovery system. *International Journal of Engineering & Science Research*, 2 (5), 318-327.

Nada S.A., Eid E.I., Abd El Aziz G.B., Hassan H.A., 2016. Performance enhancement of shell and helical coil water coolers using different geometric and fins conditions. *Heat Transfer Asian Res.*, 45, 631–647. DOI: 10.1002/htj.21180.

Naphon P., Wongwises S., 2006. A review of flow and heat transfer characteristics in curved tubes. *Renewable Sustainable Energy Rev.*, 10, 463–490. DOI: 10.1016/j.rser.2004.09.014.

Pandey A.K., Mishra P.K., Srivastava K.K., 2015. Theoretical study of single phase heat transfer in a helically coiled tube of small diameter. *IJCEA*, 6, 460–463 DOI: 10.7763/IJCEA.2015.V6.530.

Pettersen J., Rieberer R., Munkejord S.T., 2000. Heat transfer and pressure drop for flow of supercritical and subcritical $CO_2$ in microchannel tubes. Technical Report. SINTEF Energy Research, Trondheim, Norway.

Sapali S.N., Patil P.A., 2010. A new experimental technique to determine heat transfer coefficient and pressure drop in smooth and micro-fin tube. *J. Mech. Eng. Res.*, 2, 4, 71–84.

Schmidt E.F., 1967. Wärmeübergang und Druckverlust in Rohrschlangen. *Chemie Ing. Tech.*, 39, 781–789. DOI: 10.1002/cite.330391302.

Shah R., Sekulić D., 2003. *Fundamentals of heat exchanger design*. John Wiley &Sons, Inc., Hoboken.

Shiragami N., Inoue I., 1986. Pressure losses in rectangular bends, In: Cheremisinoff N.P. (Ed.), *Encyclopedia of Fluid Mechanics: Flow phenomena and measurement*. Gulf Pub. Co., Book Division, 870-895.

Silva L.F., Marczak L.D.F., Möller S.V., 2001. Determination of the local heat transfer coefficient in pipes with helical turbulence promoters through the naphthalene sublimation technique. *Lat. Am. Appl. Res.*, 31, 5, 495–500.

Sobota T., 2011. Experimental prediction of heat transfer correlations in heat exchangers, In: Dos Santos Bernardes M.A. (Ed.), *Developments in heat transfer*. *InTech.* DOI: 10.5772/20362.

Srinivasan, P.S., Nandapurkar, S.S., Holland, F.A., 1968. Pressure drop and heat transfer in coils. *The Chemical Engineer*, 218, 113–119.

Thulukkanam K., 2013. *Heat exchanger design handbook*. Second edition. *CRC Press*, Boca Raton.

Uhía F.J., Campo A., Fernández-Seara J., 2013. Uncertainty analysis for experimental heat transfer data obtained by the Wilson plot method: Application to condensation on horizontal plain tubes. *Therm. Sci.*, 17, 2, 471–487. DOI: 10.2298/TSCI110701136U.

Urbanowicz-Górska A., Wojtkowiak J., 2012. Method of heat and fluid flow calculations of vertical helical pipe immersed in cold liquid of constant temperature. Part 1. Equations and algorithm of the method. *Ciepłownictwo, Ogrzewnictwo, wentylacja*, 43, 7, 284-288.

Van Rooyen E., Christians M., Thome J.R., 2012. Modified Wilson plots for enhanced heat transfer experiments: current status and future perspectives. *Heat Transfer Eng.*, 33, 342-3-55. DOI: 10.1080/01457632.2012.611767.

Vashisth S., Kumar V., Nigam K.D.P., 2008. A Review on the Potential Applications of Curved Geometries in Process Industry. *Ind. Eng. Chem. Res.*, 47, 3291–3337. DOI: 10.1021/ie701760h.

Witchayanuwat W., Kheawhom S., 2010. Heat transfer coefficients for particulate airflow in shell and coiled tube heat exchangers. *International Journal of Chemical and Biological Engineering*, 3, 1, 7–11.

Yang R., Chiang F.P., 2002. An experimental heat transfer study for periodically varying-curvature curved-pipe. *Int. J. Heat Mass Transfer*, 45, 3199–3204. DOI: 10.1016/S0017-9310(02)00023-6.

*Received 16 May 2018*
*Received in revised form 31 December 2018*
*Accepted 21 February 2019*